He and H sequential implantation induced surface blistering and the exfoliation of Si covered with an oxide layer *

WANG Zhuo(王卓)[1,2] GAO Yu-Jie(高玉杰)[1] LI Meng-Kai(李梦凯)[1]
ZHU Fei(朱飞)[1] ZHANG Da-Cheng(张大成)[1] LIU Chang-Long(刘昌龙)[1,3;1)]

[1] School of Science, Tianjin University, Tianjin 300072, China
[2] School of Science, Tianjin University of Technology and Education, Tianjin 300222, China
[3] Tianjin Key Laboratory of Low Dimension Materials Physics and Preparing Technology, Institute of Advanced Materials Physics Faculty of Science, Tianjin 300072, China

Abstract: Si wafers with a 220 nm top oxide layer were sequentially implanted at room temperature with 40 keV He and 35 keV H ions at a fluence of $5\times10^{16}/cm^2$ and $1\times10^{16}/cm^2$, respectively. Techniques of scanning electron microscopy, atomic force microscopy and cross-sectional transmission electron microscopy (XTEM) were used to characterize the thermal evolution of surface damage as well as defect microstructures. Surface blisters as well as the localized exfoliation (∼0.42 μm in depth) have been observed for samples annealed at temperatures of 500 ℃ and above. XTEM observations reveal a variety of defect microstructures, including cavities, platelets, nanometer or micrometer sized cracks and dislocations. The platelets and cracks are mainly distributed at a depth of about 0.42 μm parallel to the sample surface, which are responsible for the occurrence of the observed surface features. The relationship between surface damage and defect microstructures is described in detail.

Key words: SiO_2/Si wafer, He and H ion implantation, localized exfoliation, crack

PACS: 61.72.Qq, 61.72.Ff, 61.82.Fk **DOI:** 10.1088/1674-1137/37/1/016001

1 Introduction

At present, the ‘smart-cut’ technology invented by Bruel [1] represents the most advanced technology to fabricate high quality silicon-on-insulator (SOI) wafers. Due to its generic nature, this technology is also applicable to other engineered substrates for the microelectronic industry such as GaAs, InP, GaN, etc. [2–4] In order to reduce production costs, reduction of both the implant dose and thermal budget necessary for the layer transfer has been the focus of many investigations [5–7]. It has been demonstrated that besides H implantation, the introduction of additional ions, such as He, D, B and so on, could enhance surface blistering and exfoliation of such semiconductor materials [7–9]. However, the defect microstructures as well as surface damage induced by co-implantation of different ions are related to many factors, such as implant sequence, implant temperature, ratio of the implant dose and so on [6, 7, 10]. Moreover, more defects and impurities introduced into solids via co-implantation could bring difficulties to clarify the involved mechanisms of damage. Therefore, more studies should be carried out to reveal surface phenomena together with the defect microstructures by sequential implantation of various ions into a series of semiconductors.

H is a very active element. It has been generally considered that H atoms could proceed through both physical interactions (gas coalescence, pressure and fracture) and chemical interactions (bond breaking, internal surface passivation) during the thin film transfer process. Among recent research on co-implantation induced surface exfoliation, the role of H implants has been emphasized. Compared with the total dose, the dose of H implants is dominant. In this article, the Si wafers covered with a 220 nm oxide layer were sequentially implanted with 40 keV He and 35 keV H ions. It should be mentioned that the ratio of implanted He ions to H ions has been fixed to be 5 to 1. With a higher He dose, the thermal evolution of defect microstructures as well as surface damage may present some differences. We have focused on the effects of He implants on the thermal evolution of defect microstructures. Moreover, the positive role of H implants has also been considered. It is shown that the

Received 10 January 2012
∗ Supported by National Natural Science Foundation of China (10975107) and Foundation of Tianjin High School Science and Technology Planning Project (20100911)
1) E-mail: liuchanglong@tju.edu.cn
©2013 Chinese Physical Society and the Institute of High Energy Physics of the Chinese Academy of Sciences and the Institute of Modern Physics of the Chinese Academy of Sciences and IOP Publishing Ltd

formation of pressurized cracks results in the appearance of surface damage, such as blistering and exfoliation.

2 The experiment

The study was performed for the (100)-oriented n-type Cz-grown Si wafers (resistivity of 3–7 Ωcm) with a 220 nm top SiO_2 surface layer (labeled as SiO_2/Si). The SiO_2 layer was grown on the Si wafer by means of a thermal oxidation process at 1150 ℃ in wet oxygen ambient for 1 h. The wafers were first implanted at room temperature with 40 keV He ions at a dose of $5\times10^{16}/cm^2$ in order to create a band of He bubbles around the ion range. Some of the He-implanted SiO_2/Si wafers were then subjected to the implantation of 35 keV H ions at a dose of $1\times10^{16}/cm^2$. Simulations from the SRIM code [11] show that the implantation of 40 keV He and 35 keV H ions into the SiO_2/Si samples provides a coincident mean projected range R_p of about 360 nm. After implantation, the wafers were cut into small pieces and used for the measurements of various techniques. Before the analyses, the sample pieces were subjected to furnace annealing in a temperature range from 400 to 1000 ℃. The annealing was conducted in a flow of nitrogen gas for 1 h.

Scanning electron microscopy (SEM) was used to characterize the surface morphology as well as its thermal evolution. The SEM images were taken using a JEOL model JSM 6700 F microscopy with a field-emission gun, operating at 10 kV. Moreover, in order to acquire more information on surface structures, atomic force microscopy (AFM) observations were also performed to quantitatively evaluate the thickness of the exfoliated layer as well as the sizes and heights of blisters. Finally, cross-sectional transmission electron microscopy (XTEM) investigations were made for some of the implanted and annealed samples to identify the defect microstructures. Before XTEM observations, the samples were cut, glued, and then thinned using mechanical polishing and ion milling. XTEM images were taken at 200 kV with a JEOL 2010 microscopy.

3 Results

First, it is worth mentioning that the SEM and AFM investigations have been made for the SiO_2/Si samples singly implanted with 40 keV He ions at a dose of $5\times10^{16}/cm^2$. No surface features, such as blistering, exfoliation, etc., are clearly observed even after 1000 ℃ annealing. However, by using sequential implantation of He and H ions, subsequent annealing causes a series of surface modifications on the SiO_2/Si samples at temperatures of 500 ℃ and above, as presented in Fig. 1. At 500 ℃ annealing, few craters could be occasionally observed (Fig. 1(a)). When annealing was performed at 700 ℃, more craters were produced on the sample surface (see Fig. 1(b)), indicating that the degree of surface

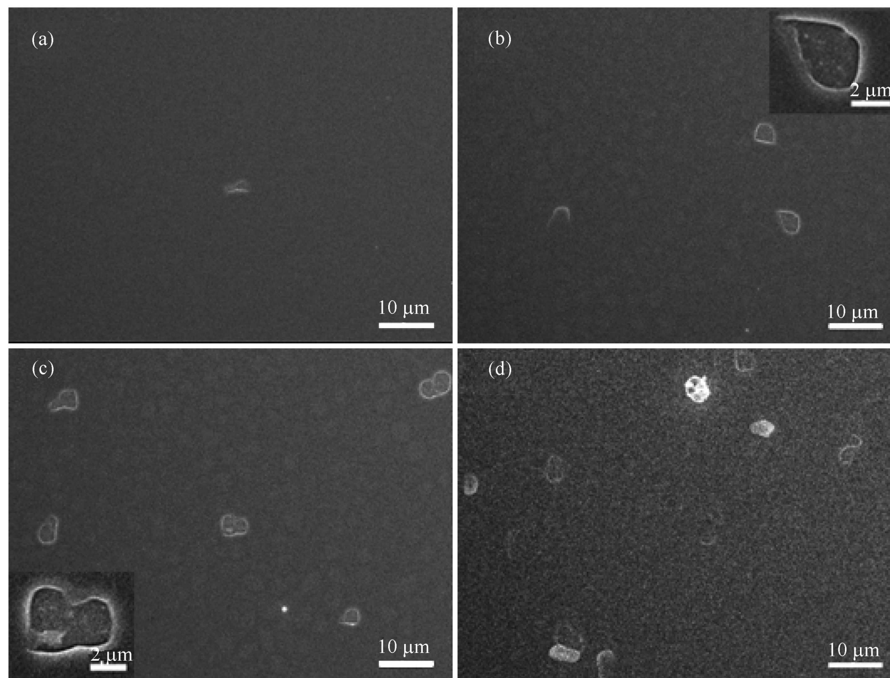

Fig. 1. SEM images taken on the SiO_2/Si samples sequentially implanted with 40 keV, $5\times10^{16}/cm^2$ He ions and 35 keV, $1\times10^{16}/cm^2$ H ions, and followed by annealing at different temperatures of (a) 500 ℃, (b) 700 ℃, (c) 800 ℃, and (d) 1000 ℃.

exfoliation increases. Moreover, blisters in high density but with a low height are also detected on the sample surface. Although the craters usually show an irregular shape, with a close look at the craters, one can find circular features at the bottom. Therefore, this suggests that the craters directly result from the broken blister domes. Further increasing annealing temperatures to 800 ℃ and 1000 ℃ give rise to the growth of blisters, and thus craters in larger sizes are observed, as shown in Fig. 1(c) and Fig. 1(d), respectively. The formation of craters in larger sizes upon high temperature annealing is mainly due to the fact that blisters tend to grow and coalesce with the neighbor ones. As an example, the inserted SEM image in Fig. 1(c) presents one large crater resulting from the rupture of a cluster of two blisters.

Formation of surface blisters and the localized exfoliation areas (craters) on the He and H implanted and annealed SiO_2/Si samples are additionally confirmed by means of AFM investigations. Fig. 2 gives the typical AFM images as well as the quantitative result on the exfoliated thickness for the He and H ion implanted SiO_2/Si samples after annealing at three different temperatures. From these images, one can see that besides the appearance of craters from the broken blister domes, blisters in large quantities are distributed throughout the sample surface upon annealing at temperatures of 500 ℃ and above. Both the heights and sizes of the blisters are found to increase with the increase in annealing temperature. Detailed measurements show that the craters have a coincident depth of about 420 nm from the sample surface, which is slightly larger than the mean projected range R_{p} of He or H ions according to the SRIM simulations [11]. As an example, the figure inserted in Fig. 2(b) gives the AFM measurement result showing the depth of one of the craters observed on the He and H implanted SiO_2/Si sample after 800 ℃ annealing.

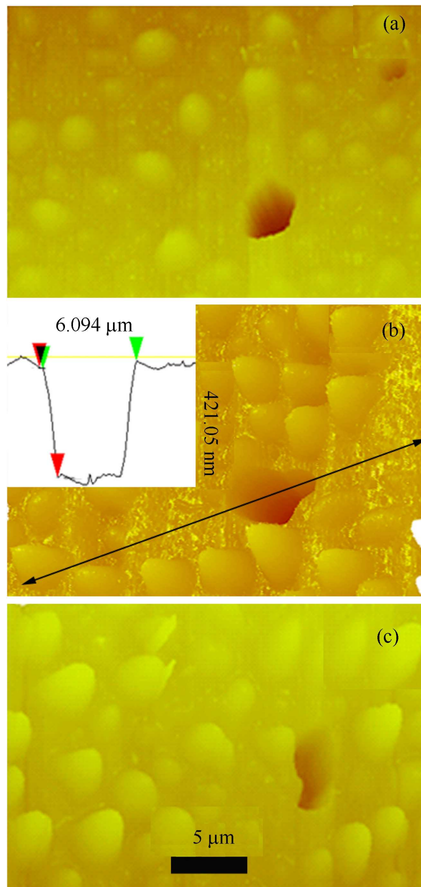

Fig. 2. AFM results obtained on the SiO_2/Si samples sequentially implanted with 40 keV, $5\times10^{16}/cm^2$ He ions and 35 keV, $1\times10^{16}/cm^2$ H ions, and followed by annealing at different temperatures of (a) 500 ℃, (b) 800 ℃, and (c) 1000 ℃.

In order to understand the involved mechanism for the observed surface damage, XTEM observations have been carried out for some of the implanted and annealed SiO_2/Si samples. As shown in Fig. 3, a well-defined defect band was created after 40 keV He-only implantation and subsequent 800 ℃ annealing. The band is located at a depth range of 220 to 420 nm from the surface, which mainly consists of the isolated cavities and dislocation-like defects. The cavities usually show a spherical shape and have sizes in the range from 4.0 to 25.0 nm with an average size of about 11.0 nm. No cavities have clearly been observed in the top SiO_2 surface layer.

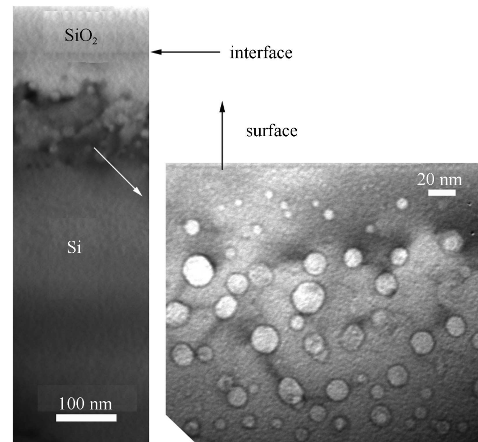

Fig. 3. XTEM micrographs of the SiO_2/Si sample singly implanted with 40 keV He ions at a dose of $5\times10^{16}/cm^2$ and followed by annealing at 800 ℃ for 1 h.

XTEM observations demonstrate much more complicated defect microstructures in He and H sequentially implanted and the 800 ℃ annealed SiO_2/Si sample, as presented in Fig. 4. Similar to that observed in He singly implanted and the 800 ℃ annealed sample (Fig. 3), the implantation of He and H ions together with 800 ℃ annealing also generates a well-defined defect band located

at a depth of 220 to 420 nm from the sample surface (Fig. 4(a)). A close view of the defect band has identified a variety of defect microstructures. Firstly, the defect band generally consists of the isolated cavities and dislocations, as shown in Fig. 4(b). The cavities are usually round and have sizes in the range of 4–11 nm with an average value of about 6 nm. Compared with that of He-only implantation (Fig. 3), it is obvious that the mean size of cavities reduces significantly. Secondly, cracks in nanometer and micrometer sizes as well as the elongated cavities in large size (larger than 50 nm) are also found in some regions of the defect band, which mainly distribute at the bottom of the defect band, i.e. at a depth of about 420 nm from the sample surface (see Fig. 4(c)). It should be emphasized that such depth is nearly the same as the thickness of the exfoliated layer measured by means of AFM (see Fig. 2(a)). Thirdly, the sample layers above the micro-cracks are not flat, and usually show obvious curvature, indicating that the formation of cracks in micrometer size is responsible for the occurrence of surface blisters, and even for that of the localized exfoliation.

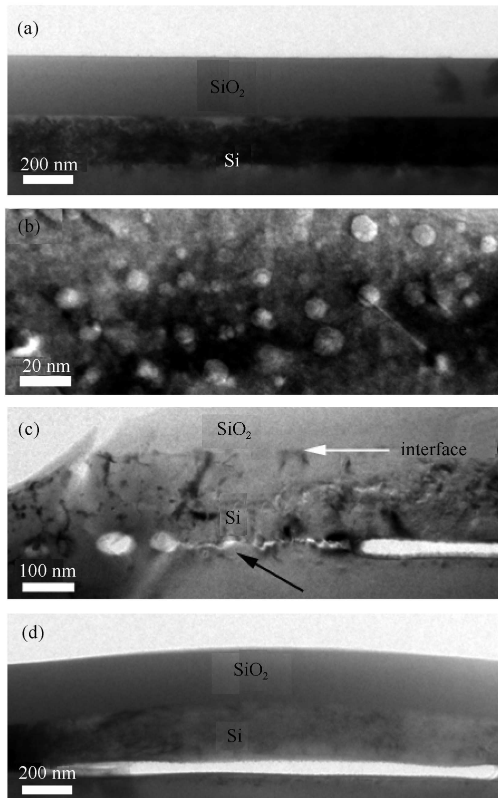

Fig. 4. XTEM images of the SiO_2/Si sample by sequential implantation of 40 keV, 5×10^{16}/cm^2 He ions and 35 keV, 1×10^{16}/cm^2 H ions and annealing at 800 ℃ for 1 h, (a) an overall defect morphology, (b) a close view of the isolated cavities, (c) a close view of cracks around the ion range, and (d) the image showing the lift of the sample surface above one micro-crack.

As an example, Fig. 4(d) gives a typical XTEM image showing surface lift above one micro-crack formed in Si bulk.

Apart from the above-mentioned defect morphologies, H platelets could also be found in the defect band. Fig. 5 presents the typical XTEM micrograph showing some of the platelets (highlighted by circles) formed in the SiO_2/Si sample by He and H co-implantation and 800 ℃ annealing. It is obvious that the platelets are also produced in the sample region near the bottom of the defect band, which is nearly parallel to the sample surface.

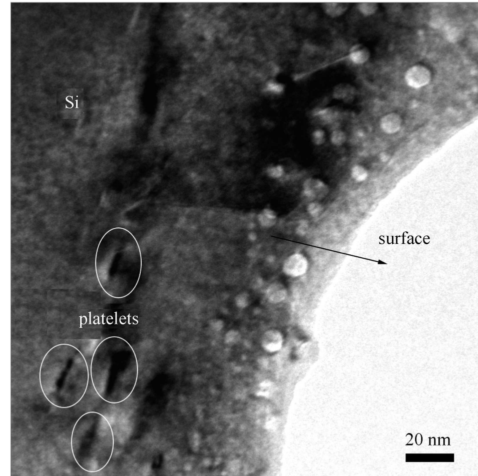

Fig. 5. The XTEM image showing the formation of platelets in the SiO_2/Si sample sequentially implanted with 40 keV He ions at a dose of 5×10^{16}/cm^2 and 35 keV H ions at a dose of 1×10^{16}/cm^2, and followed by 800 ℃ annealing.

4 Discussion

It has been indicated experimentally and theoretically [12, 13] that the onset of blistering or exfoliation needs the formation of pressurized cracks with a critical size D_c. When the critical size is reached, the stress induced by the gas pressure overcomes the over layer strength of the cracks, causing its lift above the original sample surface, then appearing as localized blisters or even as exfoliated regions resulting from broken blister domes. For the SiO_2/Si samples singly implanted with 40 keV He ions (see Fig. 3), although a band of nanometer sized cavities is created upon annealing, the cavities are usually small and distributed quite discretely. Thus, no surface features of blisters and the localized exfoliation areas should be expected for He only implanted SiO_2/Si samples even after high temperature annealing.

However, situations are quite different for the SiO_2/Si samples by sequential implantation of He and H ions and annealing. Our XTEM observations clearly show that

additional H ion implantation largely modifies the defect microstructures in He pre-implanted SiO_2/Si samples upon high temperature annealing. The micro-defects, including elongated cavities, platelets and cracks in nanometer and micrometer sizes are effectively created, which are mainly distributed at a depth of 420 nm, slightly larger than the ion range $R_p \sim 360$ nm. Moreover, the surface blisters related cracks in micrometers are also revealed, indicating the surface features of blisters and localized exfoliation areas directly result from pressurized cracks in micrometer size. The formation and deeper location of cracks in the He and H ions are sequentially implanted and annealed SiO_2/Si samples could be attributed to the synergistic role of He and H implants in micro-defect evolution, as discussed in the following.

At first, we will emphasize the formation of cracks via the interactions of H with the implant-induced defects. H is known to be very active. When H ions are implanted into Si, H is preferentially trapped at various implantation induced lattice defects like vacancies or silicon interstitials. The occupation of bond-centered sites by H in Si crystal results in the formation of the extended H-terminated internal (100) or (111) surfaces (platelets) upon annealing, which serve to trap H_2, causing the buildup of internal pressure. The presence of such silicon hydride structures could weaken the bonding between Si atoms and could also passivate any dangling Si bonds, which in turn reduces the fracture strength of Si. If the thermal budget is sufficiently high, these platelets could coalesce, leading to the formation of nanometer or even micrometer sized cracks. The formation and evolution of platelets in H ion implanted or He and H ion co-implanted and annealed Si have been widely reported and discussed, especially in the case of low temperature annealing [14–16]. Among this research, the platelets have been generally reported to be produced in the middle part of the defect layer, where the high density of H atoms and defects could be presented. However, according to our XTEM observations (see Fig. 5), (100) platelets are created, mainly distributed at the bottom of the defect band. This result seems quite surprising. We suggest that the shift of the platelets to the deeper sample region may be attributed to the following two factors. One is the presence of a high density of defects induced by He pre-implantation. Since the H implantation is conducted after He implantation, the pre-implantation of He ions unavoidably introduces large quantities of defects (mainly pressurized bubbles) together with a large strain field surrounding them. The increased damage leads to stress relieving defect migration in the depth region of maximum damage and thus to the decrease of the elastic out-of-plane strain at this depth. Moreover, the increased damage toughens the material against fracture and the H_2-gas bubbles. Both the He-gas and H-gas bubbles could exert compressive stress on the lattice surrounding them. This stress exerts a crack closing force on other bubbles. Therefore, in the present study, owing to the pre-implantation of the He ion at a high dose, the presence of sufficient bubbles effectively shields the crack by reducing the overall stress being applied to the crack tip of H-gas bubbles that would have served as the nuclei for fracture. The shielding effect will be maximized for cracks very close to the peak in the damage distribution, i.e. the middle of the defect band. So the location of cracks in micrometer size moves to a depth beyond the mean projected range of He or H ions, where the fracture toughness is low, and the implantation damage is high enough for H-platelet formation. The dependence of crack formation depth on damage concentration has already been demonstrated by Höchbauer et al. [17] using H implantation into Si at different doses. The other factor may be related to the role of the top oxide layer in the diffusion of gas atoms (He and H or H_2) upon annealing. The presence of the oxide layer has been shown to act as an effective barrier to He diffusion towards the surface during subsequent annealing [18]. Thus, those blocked He atoms will diffuse inward and be then recaptured by bubbles, leading to the formation of over-pressurized bubbles in the damage region close to the original interface. Such over-pressurized bubbles inhibit the combination of the H with them, and thus in-diffusion of H may occur, leading to H platelets which are formed in the deep damage region owing to the presence of less over-pressurized bubbles there. Additionally, it should be pointed out that our XTEM observations show the formation of fine cracks, nanometers in size, at the bottom of the defect band (as indicated by black arrow), which may be the direct evidence for the formation of cracks via the growth of H platelets.

We then discuss the formation of cracks by emphasizing the role of He implantation in the evolution of micro-defects. It has been well demonstrated by many researchers [19–21] that a high dose He ion implantation into Si could generate a band of bubbles around the ion range. Subsequent annealing causes the growth of bubbles into cavities, accompanied by He permeation from the bubbles towards the sample surface. Thermal growth of bubbles via Ostwald ripening is mainly achieved by exchanging both the gas atoms and implant induced vacancies. In the present study, the pre-implantation of 40 keV He ions at a high dose into SiO_2/Si creates a band of bubbles around the ion range. Subsequent implantation of 35 keV H ions introduces H atoms and additional vacancy-like defects in the He bubble region owing to the same range of H ions as He ions. Since the growth of bubbles is mainly accomplished by exchanging both gas atoms and vacancies upon annealing, introduction of additional gas atoms and vacancy-like defects

would promote the thermal growth of bubbles, leading to the formation of cavities in larger sizes, or even of two continuous internal surfaces (cracks) due to intersection of the cavities in larger sizes. The promotional role of an additional H implant in the growth of the He bubbles has actually been demonstrated by our earlier study [22], in which large cavities are formed throughout the defect band owing to additional H plasma implantation and subsequent annealing. However, in this study, our XTEM observations show that the average size of cavities in the band reduces (Fig. 4(b)). Only a few elongated cavities in larger sizes (>50 nm) are produced at the bottom of the band (Fig. 4(c)), suggesting that the promotion effect preferentially appears at the deep side of the band. We consider that at least two possibilities are responsible for such an abnormal growth effect of He bubbles. One is directly associated with the He diffusion upon annealing. As mentioned above, the presence of an oxide layer on the Si surface blocks the He effusion from the bubbles at the initial annealing stage, and causes the formation of over-pressurized bubbles. Upon further annealing, He gas would be released from the bubbles, and preferentially move to the H region, resulting in the growth of bubbles there. Experimentally, the thermal motion of He towards the H region has been well explained in He and H co-implanted Si by several authors [16, 23]. The other one may be associated with the diffusion of vacancies upon annealing. Thermal annealing is known to dissolve the smaller bubbles into gas atoms together with vacancies. The vacancies ejected from the smaller bubbles could be captured by larger stable bubbles, resulting in the effective growth of them. By comparing the mean size of the cavities (∼11 nm) formed in He only implanted and 800 ℃ annealed SiO_2/Si with that (∼6 nm) observed in He, H sequentially implanted and 800 ℃ annealed samples (see Fig. 3 and Fig. 4(b)), one can clearly see that with the presence of He and H together in the defect band, the mean size of cavities reduces significantly, suggesting that there exists a remarkable loss of He and vacancies in the He bubble region. The result also provides evidence that more He and vacancies take part in the thermal evolution of defects in the region around the end of the defect band, leading to the formation of elongated cavities and/or cracks there.

5 Conclusions

In summary, by using successive implantation of 40 keV, $5\times10^{16}/cm^2$ He and 35 keV, $1\times10^{16}/cm^2$ H ions into SiO_2/Si samples, the surface features, such as blisters and the localized exfoliation, have been well explained upon annealing at temperatures of 500 ℃ and above. Localized exfoliation has been found to occur at a sample depth of about 420 nm, which is slightly larger than the mean projected range of He or H ions (R_p ∼360 nm). According to the XTEM observations, the observed surface features directly result from the formation of pressurized cracks in micrometer size. The formation of cracks at a depth slightly larger than R_p has been shown to probably be associated with the synergistic role of He and H implants in the evolution of micro-defects. Moreover, two approaches have been proposed to interpret the formation of the micro-cracks together with deeper locations by emphasizing the unique role of H or He implantation in the evolution of defect microstructures, i.e. an intersection of large cavities owing to the promotion effects of H implant on He bubble growth, and platelets act as the precursors of highly pressurized H_2-gas bubbles.

References

1 Bruel M. Electron. Lett., 1995, **31**: 1201
2 CHEN P, DI Z F, Nastasi M et al. Appl. Phys. Lett., 2008, **92**: 202107
3 Moutanabbir O Scholz R Senz S et al. Appl. Phys. Lett., 2008, **93**: 031916
4 Woo H J, Choi H W, Kim G D et al. Surf. Coat. Technol., 2009, **203**: 2370
5 Lagahe-Blanchard C, Sousbie N, Sartori S et al. Proc. Electrochem. Soc., 2003, **19**: 346
6 Nguyen P, Bourdelle K K, Maurice T et al. J. Appl. Phys., 2007, **101**: 033506
7 Agarwal A, Haynes T E, Venezia V C et al. Appl. Phys. Lett., 1998, **72**: 1086
8 Desrosiers N, Terreault B. Appl. Phys. Lett., 2006, **89**: 151922
9 MA X B, DU X F, LIU W L et al. J. Vac. Sci. Technol. B, 2009, **27**: 1063
10 Lee J K, Nastasi M, David Theodore N et al. J. Appl. Phys., 2004, **96**: 280
11 Ziegler J F, Biersack J P. SRIM (Stopping and Range of Ions in Matter) computer code (http://www.srim.org)
12 HUANG L J, TONG Q Y, CHAO Y L et al. Appl. Phys. Lett., 1999, **74**: 982
13 FENG X Q, HUANG Y. Int. J. Solids Struct., 2004, **41**: 4299
14 Nastasi M, Höchbauer T, Lee J K et al. Appl. Phys. Lett., 2005, **86**: 154102
15 Reboh S, Mattos A A, Barbot J F et al. J. Appl. Phys., 2009, **105**: 093528
16 Weldon M K, Marsico V E, Chabel Y J et al. J. Vac. Sci. Technol. B, 1997, **15**: 1065
17 Höchbauer T, Walter K C, Schwarz R B et al. J. Appl. Phys., 1999, **86**: 4176
18 LIU C L, WANG Z, LI M K et al. J. Phys. D. Appl. Phys., 2008, **41**: 135108
19 Griffioen C C, Evans J H, De Jong P C et al. Nucl. Instrum. Methods B, 1987, **27**: 417
20 Raineri V, Saggio M, Rimini E. J. Mater. Res., 2000, **15**: 1449
21 Cerofolini G F, Corni F, Frabboni G et al. Mater. Sci. Eng. R, 2000, **27**: 1
22 LIU C L, Ntosenzok E, Vengurlekar A et al. J. Vac. Sci. Technol. B, 2005, **23**: 990
23 DUO X Z, LIU W L, ZHANG M et al. J. Appl. Phys., 2001, **90**: 3780